

- [3] J.-D. Boissonnat, A. Cérèzo, and J. Leblond, "Shortest paths of bounded curvature in the plane," in *Proc. 1992 IEEE Int. Conf. Robot. Automat.*, Nice, France, May 1992, pp. 2315–2320.
- [4] P. Souères and J.-P. Laumond, "Shortest paths synthesis for a car-like robot," *IEEE Trans. Automat. Contr.*, vol. 41, no. 5, pp. 672–688, May 1996.
- [5] W. Nelson, "Continuous steering-function control of robot carts," *IEEE Trans. Ind. Electron.*, vol. 36, no. 3, pp. 330–337, Aug. 1989.
- [6] Y. Kanayama and B. Hartman, "Smooth local path planning for autonomous vehicles," in *Proc. IEEE Int. Conf. Robot. Automat.*, Scottsdale, AZ, May 1989, vol. 3, pp. 1265–1270.
- [7] H. Delingette, M. Hébert, and K. Ikeuchi, "Trajectory generation with curvature constraint based on energy minimization," in *Proc. IEEE/RSJ Int. Conf. Intell. Robots Syst.*, Osaka, Japan, Nov. 1991, pp. 206–211.
- [8] J.-D. Boissonnat, A. Cérèzo, and J. Leblond, "A note on shortest paths in the plane subject to a constraint on the derivative of the curvature," INRIA, Rocquencourt, France, Tech. Rep. 2160, 1994.
- [9] A. Scheuer and C. Laugier, "Planning sub-optimal and continuous-curvature paths for car-like robots," in *Proc. 1998 IEEE/RSJ Int. Conf. Intell. Robots Syst.*, Victoria, BC, Canada, Oct. 1998, pp. 25–31.
- [10] T. Kito, J. Ota, R. Katsuki, T. Mizuta, T. Arai, T. Ueyama, and T. Nishiyama, "Smooth path planning by using visibility graph-like method," in *Proc. IEEE Int. Conf. Robot. Automat.*, Taipei, Taiwan, R.O.C., 2003, pp. 3770–3775.
- [11] T. Fraichard and A. Scheuer, "From Reeds and Shepp's to continuous-curvature paths," *IEEE Trans. Robotics*, vol. 20, no. 6, pp. 1025–1035, Dec. 2004.
- [12] J. Reuter, "Mobile robots trajectories with continuously differentiable curvature: An optimal control approach," in *Proc. 1998 IEEE/RSJ Int. Conf. Intell. Robots Syst.*, Victoria, BC, Canada, Oct. 1998, vol. 1, pp. 38–43.
- [13] C. Guarino, L. Bianco, A. Piazzoli, and M. Romano, "Smooth motion generation for unicycle mobile robots via dynamic path inversion," *IEEE Trans. Robotics*, vol. 20, no. 5, pp. 884–891, Oct. 2004.
- [14] A. Piazzoli, C. Guarino Lo Bianco, M. Bertozzi, A. Fascioli, and A. Broggi, "Quintic G²-splines for the iterative steering of vision-based autonomous vehicles," *IEEE Trans. Intell. Transport. Syst.*, vol. 3, no. 1, pp. 27–36, Mar. 2002.
- [15] C.-C. Hsiung, *A First Course in Differential Geometry*. Cambridge, MA: International Press, 1997.
- [16] B. A. Barsky and J. C. Beatty, "Local control of bias and tension in beta-spline," *Comput. Graph.*, vol. 17, no. 3, pp. 193–218, 1983.
- [17] P. Lucibello and G. Oriolo, "Stabilization via iterative state steering with application to chained-form systems," in *Proc. 35th IEEE Conf. Decision Contr.*, Kobe, Japan, Dec. 1996, vol. 3, pp. 2614–2619.
- [18] A. Piazzoli, C. Guarino Lo Bianco, and M. Romano, "Smooth path generation for wheeled mobile robots using η^3 -splines," Università di Parma, Dipt. Ingegneria dell'Informazione, Parma, Italy, Tech. Rep. TSC01/07, 2007.
- [19] C. Guarino Lo Bianco and A. Piazzoli, "Optimal trajectory planning with quintic G²-splines," in *Proc. IEEE Intell. Veh. Symp. (IV2000)*, Dearborn, MI, Oct. 2000, pp. 620–625.
- [20] J. Peters, "Geometric continuity," in *Handbook of Computer Aided Geometric Design*, G. Farin, J. Hoschek, and M.-S. Kim, Eds. Amsterdam, The Netherlands: North-Holland, 2002, pp. 193–229.
- [21] C. Guarino Lo Bianco, A. Piazzoli, and M. Romano, "Smooth control of a wheeled omnidirectional robot," presented at the IFAC Symp. Intell. Autonom. Veh., IAV2004, Lisbon, Portugal, Jul. 2004.
- [22] J. Villagra and H. Mounier, "Obstacle-avoiding path planning for high velocity wheeled mobile robots," presented at the IFAC World Congr., Prague, Czech Republic, Jul. 2005.

Cooperative Motion Control and Sensing Architecture in Compliant Framed Modular Mobile Robots

Xiaorui Zhu, Youngshik Kim, Roy Merrell, and Mark A. Minor

Abstract—A novel motion control and sensing architecture for a two-axle Compliant Framed wheeled Modular Mobile Robot (CFMMR) is proposed in this paper. The CFMMR is essentially a cooperative mobile robotic system with complex physical constraints and highly nonlinear interaction forces. The architecture combines a kinematic controller for coordinating motion and providing reference commands, robust dynamic controllers for following these commands and rejecting disturbances, and a sensor fusion system designed to provide accurate relative posture estimates. Requirements for each of these subsystems and their respective interconnections are defined in this paper in order to optimize system performance. Experimental results compare performance of the proposed architecture to sub-optimal configurations. Results derived from seven groups of experiments based upon 35 individual tests validate superiority of the architecture.

Index Terms—Cooperative systems, distributed control, motion control, robot sensing systems, tracking.

I. INTRODUCTION

Cooperative motion control and sensing for Compliant Framed wheeled Modular Mobile Robots (CFMMR) (Fig. 1) is the focus of this research. The CFMMR uses compliant frame members to couple rigid axle modules with independently controlled wheels [1]. Wheel commands are used to deform the frame for advanced steering capability. Frame compliance also allows the robot to twist its shape and adapt to rugged terrain. Simplicity and modularity of the system emphasize its cost effectiveness, durability in adverse climates, and capability to be reconfigured for a multitude of applications.

A number of cooperative wheeled mobile robots have been investigated in recent decades. A detailed comparison is described in [1], [2]. Most similar of these is the snake-like robot Genbu [3], which uses entirely passive joints to allow cooperation amongst wheel axles for adaptation to uneven terrain. However, motion control of [3] focused on the simple posture alignment and functional ability [3], [4] while this paper deals with general navigation issues and accurate motion control.

In this paper, we propose a new sensing and control architecture in order for the system to be scalable, distributed, and cooperative. The architecture (Fig. 2) consists of kinematic (K) control, dynamic (D) control, and sensing (S) systems components. In this architecture, each axle module is treated individually as an autonomous mobile

Manuscript received September 5, 2006; revised January 9, 2007. This paper was recommended for publication by Associate Editor S. Ma and Editor H. Arai upon evaluation of the reviewers' comments. This work was supported by the National Science Foundation under NSF Grant IIS-0308056. This paper was presented in part at the International Conference on Robotics and Automation, Orlando, FL, 2006, and in part at the International Conference on Advanced Intelligent Mechatronics, Monterey, CA, 2005.

X. Zhu was with the Department of Mechanical Engineering, University of Utah, Salt Lake City, UT 84112 USA. She is now with Harbin Institute of Technology at Shenzhen, Shenzhen, Guangdong 518055, China (e-mail: xiaorui.zhu@hitzs.edu.cn)

Y. Kim and M. A. Minor are with the Department of Mechanical Engineering, University of Utah, Salt Lake City, UT 84112 USA (e-mail: youngshik.kim@utah.edu; minor@mech.utah.edu).

R. Merrell was with the Department of Mechanical Engineering, University of Utah, Salt Lake City, UT 84112 USA. He is now with ATK Launch Systems, Magna, UT 84044 USA (e-mail: mailroy@excite.com).

Color versions of one or more of the figures in this paper are available online at <http://ieeexplore.ieee.org>.

Digital Object Identifier 10.1109/TRO.2007.903815

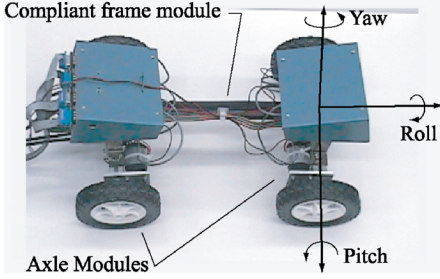


Fig. 1. Two-axle CFMMR experimental configuration.

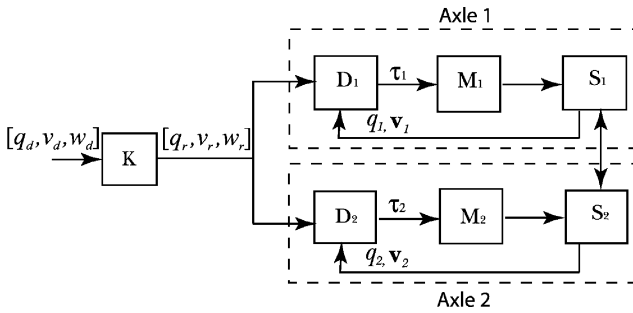


Fig. 2. Distributed sensing and control configurations where K represents kinematic motion control, D represents dynamic motion control, S represents sensory system, and M represents each module of the robot.

robot unit. Thus, identical algorithms can be applied to each unit of the system, which provides naturally distributed computational burden. Compliant coupling complicates this task, however, since each axle imposes boundary conditions on its neighboring compliant frame elements and resulting interaction forces are created.

In order to reduce interaction forces in lieu of nonholonomic constraints, axle cooperation is managed via centralized kinematic control. Based on ideal kinematics, the kinematic controller considers frame boundary conditions and provides bounded posture and velocity commands such that the system follows a reference trajectory or regulates to a final posture asymptotically. The distributed dynamic controllers then track these reference commands such that physical constraints are satisfied during movement of the robot in lieu of disturbances. Since off-tracking between neighboring axles can increase interaction forces, the distributed sensing system includes a relative position sensor within a tiered fusion algorithm to provide accurate posture and velocity estimates.

Motion control of wheeled mobile robots has received appreciable attention in recent years, where rigid axle wheeled mobile robots are predominant platforms. In earlier stages, most research was based on the kinematic model of a wheeled mobile robot where the input is velocity [5], [6]. However, tracking the velocity commands with an actual robot and rejecting the resulting drift is not trivial. Thus, the uniform dynamic controllers derived in [7], [8] were based on the kinematic and dynamic model of the robot such that the robot can be controlled using wheel torque commands. Motion control of the CFMMR, however, is different in two aspects. First, the physical constraints, especially the axle velocity and curvature constraints imposed by the frame, are not typical in rigid body wheeled mobile robots that are the focus of the uniform dynamic controllers. Second, the interaction forces between the axles are highly nonlinear functions of relative axle postures. Thus, coordinating relative axle postures is a critical concern that is not considered by the uniform dynamic controllers mentioned above. In contrast, the motion control architecture proposed here is ideal for coordinating motion of the axles in lieu of interaction constraints.

Coordination is a common issue in cooperative mobile robotics, and has been considered with a variety of techniques [9]–[14]. Some of them only focus on motion planning and coordination issues without sensor architecture involved [11], [14]. Some only consider motion planning and sensor architecture ignoring robot dynamics [9], [13]. Others only focus on dynamic motion control and coordinated force control without considering motion planning and sensor issues [10], [12], [15]. None of them consider the combination of motion planning, dynamic motion control and complex sensor fusion. There is no general solution to resolve all three aspects. In reality, motion planning, dynamic control and sensor architecture issues, however, all affect efficiency of cooperative motion control.

Burdick and his students proposed controllability and motion planning issues for multimodel systems including overconstrained wheeled vehicles where conventional nonholonomic motion planning and control theories do not apply [16]. They developed a power dissipation method (PDM) and talked about the conditions of kinematic reducibility for such systems. Then the solutions of PDM were shown actually as the solutions of kinematic reducibility. The PDM technique was provided to simplify motion control analysis from the full Lagrangian mechanical framework. As they stated, however, the full Lagrangian still plays an important role in analyzing mechanical systems in general. While the CFMMR has similarities to overconstrained wheeled vehicles, this paper provides a motion control and sensing architecture based on the general full Lagrangian analysis to accommodate the conventional nonholonomic control theories onto the cooperative nonholonomic system.

The main contributions of this paper involve a distributed cooperative motion control and sensing architecture. The architecture and requirements for the kinematic controller, dynamic controller, and sensor system components are specified in order to reduce tracking error in lieu of robot interaction forces and unmodeled disturbances. The architecture provides a framework optimized for allowing previous research on the aforementioned topics to be combined to form a robust cooperative motion control system [2], [17], [18]. Therefore, algorithms and controllers previously developed for each component are implemented and the architecture is evaluated experimentally. While the target application is the CFMMR, this architecture is easily extended to any cooperative mobile robotic system, but the specific algorithms in the modules may need to be customized for a particular application. Further, given the modular structure of the architecture, it is easy to customize specific components to satisfy navigation requirements of the robot and to allow a team to design the components in parallel for faster implementation.

The structure of the paper is as follows. The generic modeling structure is presented in Section II as a foundation for sensing and control. Our overall motion control and sensing strategy is discussed for a two-axle CFMMR in Section III. The requirements and implementation of the kinematic motion controller, the dynamic motion controller, and the sensory system are presented in Sections IV–VI. The experimental evaluation is discussed in Section VII. Concluding remarks and future works are described in Section VIII.

II. GENERIC MODELING STRUCTURE

Consider the CFMMR model shown in Fig. 4, which shows two axles connected by a compliant frame member. Based on a one-axle unicycle-type wheeled robot (Fig. 3), let us define a fixed global reference frame $G(X, Y)$ and moving frames $f_i(x_i, y_i)$ attached to the points C_i at the midpoint of the i th axle, where $i = 1, 2$ (Fig. 4). At any instant, the i th axle module is rotating about the instantaneous center (IC), such that the IC's projections onto the x_i axes define point C_i at the midpoint of each axle. A module configuration vector $q_i = [x_i \ y_i \ \phi_i]$

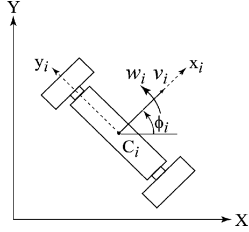
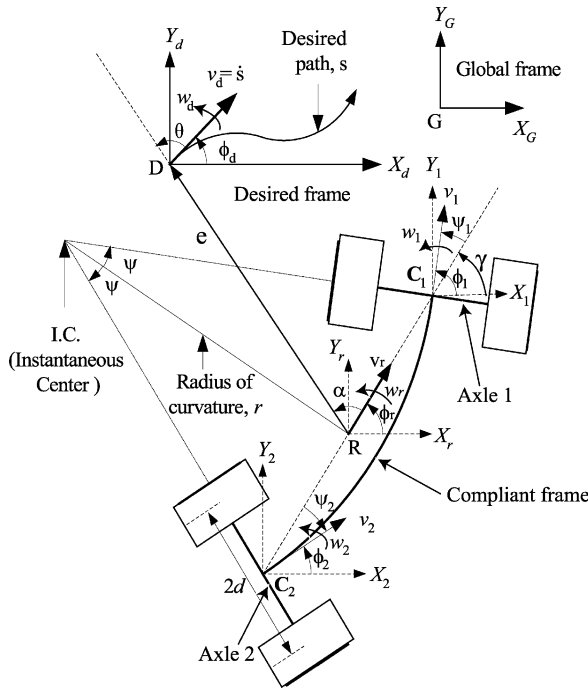
Fig. 3. The i th axle module.

Fig. 4. Two-axle CFMMR.

is then attached to this point for each axle. We then have the dynamic model

$$\mathbf{M}_i(q_i)\ddot{q}_i + \mathbf{V}_i(q_i, \dot{q}_i)\dot{q}_i + \mathbf{F}_i(\dot{q}_i) + \mathbf{G}_i(q_i) + \tau_{d,i} + \mathbf{F}_{K,i}(q_i, q_{i\pm 1}) = \mathbf{E}_i(q_i)\tau_i - \mathbf{A}_i^T(q_i)\lambda_i \quad (1)$$

where $\mathbf{M}_i(q_i) \in R^{3 \times 3}$ is a symmetric, positive definite inertia matrix for the i th axle module. $\mathbf{V}_i(q_i, \dot{q}_i) \in R^{3 \times 3}$ is the centripetal and Coriolis forces, $\mathbf{F}_i(\dot{q}_i) \in R^{3 \times 1}$ denotes the friction, $\mathbf{G}_i(q_i) \in R^{3 \times 1}$ is the gravitational vector, $\tau_{d,i}$ denotes bounded unknown disturbances including unstructured unmodeled dynamics, $\mathbf{E}_i(q_i) \in R^{3 \times 2}$ is the input transformation matrix, $\tau_i \in R^{2 \times 1}$ is the input torques, and $\lambda_i \in R^{1 \times 1}$ is the vector of nonholonomic constraint forces. $\mathbf{A}_i(q_i) \in R^{1 \times 3}$ is the global matrix associated with the nonholonomic constraints. $\mathbf{F}_{K,i}(q_i, q_{i\pm 1}) \in R^{3 \times 1}$ represents the compliant frame forces, which impose additional physical constraints dependent upon flexible beam interaction.

Physical constraints, then, include nonholonomic constraints, $\mathbf{A}_i(q_i)\dot{q}_i = 0$, imposed by the wheels and curvature and velocity constraints imposed by the compliant frame [1]. The kinematic controller acts to coordinate axle commands such that all physical constraints are satisfied *a priori*. The axle level dynamic controller is then based upon (1) in order to consider all forces acting upon the axle.

III. MOTION CONTROL AND SENSING STRATEGY

Given the two-axle CFMMR, the control objective is to solve multiple navigation problems using a general approach. These include posture regulation, path following and trajectory tracking.

Let us analyze the target system first. Compared to the traditional unicycle-type wheeled mobile robot, the CFMMR also has physical constraints imposed by the frame in addition to nonholonomic constraints. The frame also complicates the dynamics by introducing highly nonlinear compliance. Resulting forces are quite dependent on the ability of the measurement system to predict relative axle posture, and thus the data fusion and instrumentation systems must be modified to improve relative position sensing.

According to the control objective and characteristics of the CFMMR, the motion control and sensing architecture is proposed (Fig. 2). In order to characterize the performance of this architecture, the tracking errors due to the kinematic motion controller, dynamic motion controller, and sensing algorithms are defined as

$$q_r - q_d = e_k \quad q_s - q_r = e_d \quad q - q_s = e_s \quad (2)$$

where q_d is the desired trajectory according to the virtual desired frame D, $q_d = [x_d, y_d, \phi_d]$ (Fig. 4). q_r is the reference trajectory created by the kinematic controller that the dynamic motion controller refers to: $q_r = [x_r, y_r, \phi_r]$. q_s is the trajectory estimates from the sensory system, and q is the actual trajectory of the axles. Components of q_d and q_r are shown in Fig. 4. We then desire to minimize the total tracking error e_{tot} , which is expressed as

$$e_{tot} = q - q_d = e_k + e_d + e_s. \quad (3)$$

The norm of the total tracking error, $\|e_{tot}\|$, is then

$$\|e_{tot}\| = \|e_k + e_d + e_s\| \leq \|e_k\| + \|e_d\| + \|e_s\|. \quad (4)$$

Thus, to minimize the total tracking error, each component error should be minimized

$$\begin{aligned} \min(\|e_k\| + \|e_d\| + \|e_s\|) \\ = \min(\|e_k\|) + \min(\|e_d\|) + \min(\|e_s\|). \end{aligned} \quad (5)$$

In the following sections, the kinematic motion controller, dynamic motion controller, and sensory system are designed to minimize $\|e_k\|$, $\|e_d\|$, and $\|e_s\|$, respectively, in lieu of physical constraints due to the cooperative configuration, i.e., the compliant frame on CFMMR.

IV. KINEMATIC MOTION CONTROLLER

According to the proposed control architecture, the kinematic motion controller considers physical constraints and provides the reference velocity inputs to the dynamic motion controllers. As shown in Fig. 4, suppose that a desired trajectory, $q_d = [x_d, y_d, \phi_d]$, is produced by the desired linear and angular velocities, v_d and ω_d such that the path has curvature K_d . The kinematic motion controller is designed as follows.

- 1) The robot is asymptotically driven to the desired trajectory using the reference velocity inputs v_r and ω_r such that $\|e_k\| = 0$.
- 2) The path of the robot produced by the reference velocity inputs v_r and ω_r will not violate physical constraints at any point of the path. Then, the compliant frame curvature is limited to a certain value related to the physically feasible configurations. Since the compliant frame forces $\mathbf{F}_{K,i}$ are a function of the two axle postures $(q_i, q_{i\pm 1})$, they are bounded for all the robot configurations during the navigation given the kinematic motion controller.

- 3) The kinematic motion controller should be based on ideal kinematics, e.g., no feedback signal should be introduced from the actual robot since this perturbs convergence of the kinematic controller.
- 4) The compliant frame should be subjected to pure bending ($\psi = \psi_1 = -\psi_2$) (Fig. 4). This minimizes disturbance forces acting on the dynamic controller [1], and improves performance of the sensory system [18].

Polar coordinates (e, θ, α) (Fig. 4) are used to describe the reference configuration, q_r , and the reference velocity inputs are designed according to requirements 1 and 2 as

$$v_r = u_1(e, \theta, \alpha) \quad \omega_r = u_2(e, \theta, \alpha). \quad (6)$$

The controlled system then becomes

$$\begin{aligned} \dot{e} &= f_1(e, \theta, \alpha, v_r, \omega_r) = f'_1(e, \theta, \alpha) \\ \dot{\theta} &= f_2(e, \theta, \alpha, v_r, \omega_r) = f'_2(e, \theta, \alpha) \\ \dot{\alpha} &= f_3(e, \theta, \alpha, v_r, \omega_r) = f'_3(e, \theta, \alpha) \end{aligned} \quad (7)$$

where the polar configuration of the robot goes to the equilibrium point ($e = \theta = \alpha = 0$) as time goes to infinity, i.e., $\|e_k\| = 0$.

If the velocity inputs have small perturbations, $\hat{v}_r = v_r + \delta v_r$ and $\hat{\omega}_r = \omega_r + \delta \omega_r$ where $\delta v_r \neq 0$ and $\delta \omega_r \neq 0$, which happens if requirement 3 is violated, then requirement 1 cannot be guaranteed. Under the perturbed velocity input the controlled system becomes

$$\begin{aligned} \dot{\tilde{e}} &= f'_1(\tilde{e}, \tilde{\theta}, \tilde{\alpha}) + g_1(\tilde{e}, \tilde{\theta}, \tilde{\alpha}, \delta v_r, \delta \omega_r) \\ \dot{\tilde{\theta}} &= f'_2(\tilde{e}, \tilde{\theta}, \tilde{\alpha}) + g_2(\tilde{e}, \tilde{\theta}, \tilde{\alpha}, \delta v_r, \delta \omega_r) \\ \dot{\tilde{\alpha}} &= f'_3(\tilde{e}, \tilde{\theta}, \tilde{\alpha}) + g_3(\tilde{e}, \tilde{\theta}, \tilde{\alpha}, \delta v_r, \delta \omega_r) \end{aligned} \quad (8)$$

where

$$\begin{aligned} g_1(\tilde{e}, \tilde{\theta}, \tilde{\alpha}, 0, 0) &= 0 \\ g_2(\tilde{e}, \tilde{\theta}, \tilde{\alpha}, 0, 0) &= 0 \\ g_3(\tilde{e}, \tilde{\theta}, \tilde{\alpha}, 0, 0) &= 0. \end{aligned} \quad (9)$$

Then for $\delta v_r \neq 0$ and $\delta \omega_r \neq 0$, the new equilibrium point is nonzero, which violates requirement 1. The requirement 3 is therefore proven.

In order to satisfy the above requirements, a centralized kinematic motion controller is presented as [17]

$$\begin{aligned} v_r &= \frac{\left\{ k_1 e \sqrt{\zeta - \cos 2\theta} \tanh(e - r \sqrt{2} \sqrt{\zeta - \cos 2\theta}) \right.}{\left. (+v_d e \cos \theta \sqrt{\zeta - \cos 2\theta} + v_d r \sqrt{2} \sin 2\theta (\sin \theta + \kappa_d e)) \right\}} \\ \omega_r &= k_2 \tanh(\theta + \alpha) + \frac{2}{e} (v_r \sin \alpha - v_d \sin \theta) - v_d \kappa_d \end{aligned} \quad (10)$$

where r is the radius of a circular *path manifold*. $\zeta = 1 + \varepsilon$ and ε is a sufficiently small perturbation. Refer to [17] for detailed derivation of this controller.

Since the above kinematic motion controller is centralized, the cascade connection was developed to provide commands to each axle [1]. To satisfy the pure bending requirement 4, ψ may be solved numerically using the expression for the path radius of point R

$$\frac{1}{r} = \frac{2\psi}{L \cos \psi} \quad (11)$$

where L is the frame length. Hence, the linear and angular velocities of each axle, $v_{r,i}$ and $\omega_{r,i}$ are obtained by

$$\begin{aligned} v_{r,i} &= \frac{v_r}{\cos \psi} + \frac{(-1)^i}{6} L \psi \dot{\psi} \quad \left\{ \begin{array}{l} i = 1 \text{ for front axle} \\ i = 2 \text{ for rear axle} \end{array} \right. \\ \omega_{r,i} &= \omega_r + (-1)^{i-1} \dot{\psi} \end{aligned} \quad (12)$$

which satisfies physical constraints imposed by the frame.

In the centralized kinematic controller, the velocity (v_r, ω_r) of the middle point of the front and rear axle units, R , was introduced as the auxiliary centralized states (Fig. 4). These centralized states were

then passed between the axle units using the cascade connection mentioned above. The limitation of the centralized kinematic controller is that scalability of the aforementioned controller to multiaxle configurations is not trivial, which is the subject of future work [19].

V. DYNAMIC MOTION CONTROLLER

Using the proposed architecture, the dynamic motion controller provides wheel torque commands to the robot based upon the reference trajectory from the kinematic motion controller $(q_{r,i}, v_{r,i}, \omega_{r,i})$. The dynamic motion controller is designed as follows.

- 1) Dynamic motion control is distributed for scalability and reduced axle level computational burden.
- 2) Model-based frame interaction force estimates are included in the controller such that frame force disturbances on e_d are reduced.
- 3) Each axle follows the individual reference trajectories from the kinematic motion controller robustly using wheel torque commands. When the CFMMR works on rough terrain or even more complicated environments, the compliant frame forces might not be estimated accurately enough. So the dynamic motion controller should be robust and adaptive to the uncertainties caused by the complex interaction forces and the other dynamic disturbances. The trajectory tracking error should be uniformly bounded based on the bounded compliant frame forces, i.e., $\|e_d\| \leq \varepsilon_d$, $\varepsilon_d > 0$.

In order to satisfy all the three requirements, a distributed motion controller is given by [2], [17]

$$\tau_i = -(\mathbf{S}_i^T \mathbf{E}_i)^{-1} K_i \mathbf{e}_{c,i} \|\xi_i\|^2. \quad (13)$$

Here

$$\xi_i^T = \{\|\mathbf{v}_i\|, \|\mathbf{v}_i\|, \|\mathbf{v}_{r,i}\|, \|\dot{\mathbf{v}}_{r,i}\|, 1, \|\mathbf{F}_{K,i}(q_{s,i}, q_{s,i \pm 1})\|\} \quad (14)$$

$$\mathbf{e}_{c,i} = \mathbf{v}_i - \mathbf{v}_{c,i} \quad (15)$$

$$\mathbf{v}_{c,i} = \begin{bmatrix} v_{r,i} \cos e_{\phi,i} + k_{X,i} e_{X,i} \\ \omega_{r,i} + k_{Y,i} v_{r,i} e_{Y,i} + k_{\phi,i} v_{r,i} \sin e_{\phi,i} \end{bmatrix} \quad (16)$$

$$[e_{X,i} \quad e_{Y,i} \quad e_{\phi,i}]^T = \mathbf{R}_{\phi,i}(q_{r,i} - q_{s,i}) \quad (17)$$

$$\mathbf{R}_{\phi,i} = \begin{bmatrix} \cos \phi_{s,i} & \sin \phi_{s,i} & 0 \\ -\sin \phi_{s,i} & \cos \phi_{s,i} & 0 \\ 0 & 0 & 1 \end{bmatrix} \quad (18)$$

$$\mathbf{E}_i = \frac{1}{r_w} \begin{bmatrix} \cos \phi_{s,i} & \sin \phi_{s,i} & -d \\ \cos \phi_{s,i} & \sin \phi_{s,i} & d \end{bmatrix}^T \quad (19)$$

$$\mathbf{S}_i^T = \begin{bmatrix} \cos \phi_{s,i} & \sin \phi_{s,i} & 0 \\ 0 & 0 & 1 \end{bmatrix} \quad (20)$$

where ξ_i is a known, positive definite vector. $K_i = \begin{bmatrix} K_{1,i} & 0 \\ 0 & K_{2,i} \end{bmatrix}$ is the matrix control gain and $K_{1,i}$, $K_{2,i}$, $k_{X,i}$, $k_{Y,i}$ and $k_{\phi,i}$ are positive constants. $\mathbf{v}_i = [v_{s,i} \quad \omega_{s,i}]^T$ is the estimated axle velocity vector obtained from the sensory system. The r_w and d are wheel radius and half axle length, respectively (Fig. 4). $\mathbf{F}_{K,i}$ is the estimated frame force vector [2]. For the detailed derivation of these equations, refer to [2].

VI. SENSORY SYSTEM

The sensor system provides posture and velocity feedback to the dynamic motion controllers according to the proposed architecture (Fig. 5). The sensor system is designed with the following characteristics.

- 1) Independent sensors are distributed on each axle.
- 2) Cooperative sensors provide relative posture estimates between neighboring axles.

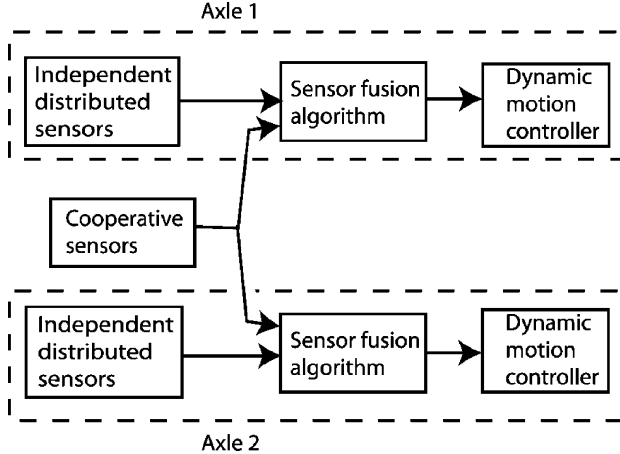


Fig. 5. Sensor fusion algorithm block diagram.

- 3) Sensor data (either independent or cooperative) is fused to minimize posture estimate error (Fig. 5), i.e., $\|e_s\| \leq \varepsilon_s$, $\varepsilon_s > 0$.
- 4) Sensor fusion is distributed for scalability and reduced axle level computational burden.

Traditional independent sensors (odometry, inertial measurements, and even GPS) fused with common model-based extended Kalman filters (EKF) provide axle posture estimates that are prone to drift and uncertainty. Such estimates are insufficient for managing cooperation amongst robots where interaction forces may occur. This is the case of the CFMMR, where frame compliance can cause large interaction forces due to drift in relative axle posture estimates. Thus, requirement 2 specifies that cooperative sensors be provided to bound relative posture estimate error.

A sensory system incorporating relative position sensors (RPSs) is presented to satisfy the above requirements [18], [20]. The cooperative RPS consists of a series of strain gauges placed at known locations along the length of the compliant frame in order to provide a strain polynomial. The relative posture (x_{RPS} , y_{RPS} , ϕ_{RPS}) of one axle to the other is calculated by piecewise integration of dx , dy , and $d\phi$. Assuming sufficiently small step size, dL , the dx , dy , and $d\phi$ can be calculated as

$$d\phi = \frac{dL}{\rho} \quad dx = \rho \sin(d\phi) \quad dy = \rho(1 - \cos(d\phi)) \quad (21)$$

where the frame radius of curvature ρ is obtained directly from the strain polynomial.

The EKF is used as the first tier of the sensor fusion algorithm in order to provide axle level posture estimates based upon independent sensors. Since these estimates will drift and provide poor relative axle posture estimates, the covariance intersection (CI) filter is used for second tier data fusion to combine EKF and RPS data to bound relative posture estimates. Identical implementations of these fusion algorithms operate on each axle module.

VII. EXPERIMENTAL EVALUATIONS

A. Methods and Procedures

The distributed cooperative motion control architecture for the two-axle CFMMR was simulated in Matlab and Simulink to adjust control gains, but the results are not shown here. Experiments were conducted on a two-module CFMMR experimental platform (Fig. 1) at the University of Utah. The robot is controlled via tether by a dSpace 1103 digital signal processor (DSP) and power is supplied externally.

Geared dc motors actuate each wheel and encoders provide position and velocity. Odometry and the relative position sensor are used in the sensing system. Two 7.2-V RC car batteries are mounted on the rear axle to power the RPS amplifying circuit. The sampling frequency of the experiments was 100 Hz in order to arrive at a compromise between the computational limits of the DSP, velocity sensor noise attributed to higher sampling rates, and robust controller chatter at lower sampling rates.

The architecture is evaluated using the algorithms presented in Sections IV–VI while performing posture regulation. The evaluations were conducted on surfaces with increasing difficulty and realism: flat carpet (C), sand (S), and sand with scattered rocks (SR). Carpet provides high traction and emphasizes the capability of the kinematic and dynamic motion controllers under ideal circumstances. Sand provides lower traction and emphasizes the importance of the sensory system. Sand-and-rock introduces difficulty and demonstrates robustness to disturbances.

Nonideal algorithms were also evaluated to justify the proposed architecture. These include a nonideal kinematic motion controller [17], a traditional backstepping dynamic motion controller [21], and a traditional odometry-based sensor system. Comparison experiments were operated on sand or carpet depending on whether controller or sensory system performance was being evaluated. The nonideal kinematic motion controller (FB) in [17] had the actual velocity fed into the kinematic controller, which does not satisfy requirement 3 in Section IV. The dynamic motion controller (NR) in [21] was not robust, which violates requirement 3 in Section V. The odometry sensor system (OD) did not have any cooperative sensors, which does not satisfy requirement 2 in Section VI.

Overall, seven experimental tests are reported with each test consisting of five trials. The initial posture of the middle point R for each test is $[x \ y \ \phi] = [-1.342 \text{ m} \ -1.342 \text{ m} \ 0^\circ]$. At the end of each trial, the final robot posture is manually measured relative to a string-grid system suspended just above the robot to determine actual final position error E and off-tracking $\Delta = \gamma - \phi$. Under ideal circumstances when pure bending is maintained, the orientation of the line $\overline{C_1 C_2}$, represented by γ , equals the actual heading angle ϕ of the velocity at point R (Fig. 4). Off-tracking Δ indicates the ability of the dynamic controller and sensor system to maintain pure bending. Standard deviations σ_E and σ_Δ are reported for manual measurements to indicate consistency. For each test, we also report position error magnitude and orientation provided by the kinematic controller $[E_k, e_k^\phi]$, dynamic controller $[E_d, e_d^\phi]$, and sensory system $[E_s, e_s^\phi]$. A successful trial is defined only if the robot can complete the posture regulation task in this trial. The success rate is defined as the number of all successful trials over the total number of trials.

B. Experimental Results and Discussion

Table I shows the final posture errors for all the tests according to odometry and manual measurements. The proposed control architecture (Tests 1, 5, 7) performs as expected. In all of these tests, the kinematic controller produces zero position error E_k and zero orientation error e_k^ϕ . Error produced by the dynamic motion controller (E_d, e_d^ϕ) and the sensor system (E_s, e_s^ϕ) both contribute to the actual error measured at the final posture. The system performance is relatively consistent with expectations. Relative to carpet (Test 1), E is increased by 80% on sand (Test 5) and 78% on sand-and-rock (Test 7). Increased disturbance is expected on these surfaces, although larger error is expected on sand-and-rock. Consistent with expectations, though, off-tracking is the least on sand. The sand allows the wheels to slip and reduce traction forces attributed to off-tracking. Overall, it can be observed from E_k , E_d , and E_s that the major source of error is produced by the

TABLE I
EXPERIMENTAL FINAL POSTURE ERROR

No.	Surf.	System kin+dyn+sens	Kinematic Contr. Err.		Dyn. Contr. Err.		Sensor Error		Actual Error		
			E_k (cm)	e_k^ϕ (deg)	E_d (cm)	e_d^ϕ (deg)	E_s (cm)	e_s^ϕ (deg)	$E \pm \sigma_E$ (cm)	$\Delta \pm \sigma_\Delta$ (deg)	Incr.err. (%)
1	C	I+I+I	0	0	1.4	9.2	9.8	0.6	9.9±1.0	-2.0±3.5	100
2	C	FB+I+I	17.3	-2.0	4.6	27.9	4.0	-36.6	21.9±0.8	30.8±8.8	121
3	C	I+NR+I	0	0	34.5	12.0	24.8	-5.2	17.5	0.6	76
4	C	I+I+OD	0	0	4.4	6.6	9.2	7.1	10.6±3.4	-8.3±4.4	7
5	S	I+I+I	0	0	0.6	13.2	18.2	-15.6	17.9±1.6	0.9±2.0	80
6	S	I+I+OD	0	0	0.5	11.0	21.3	-8.0	21.6±8.5	-8.3±18.4	21(wrt No.5)
7	SR	I+I+I	0	0	0.8	15.8	18.0	-16.2	17.6±8.3	6.1±2.2	78
											100

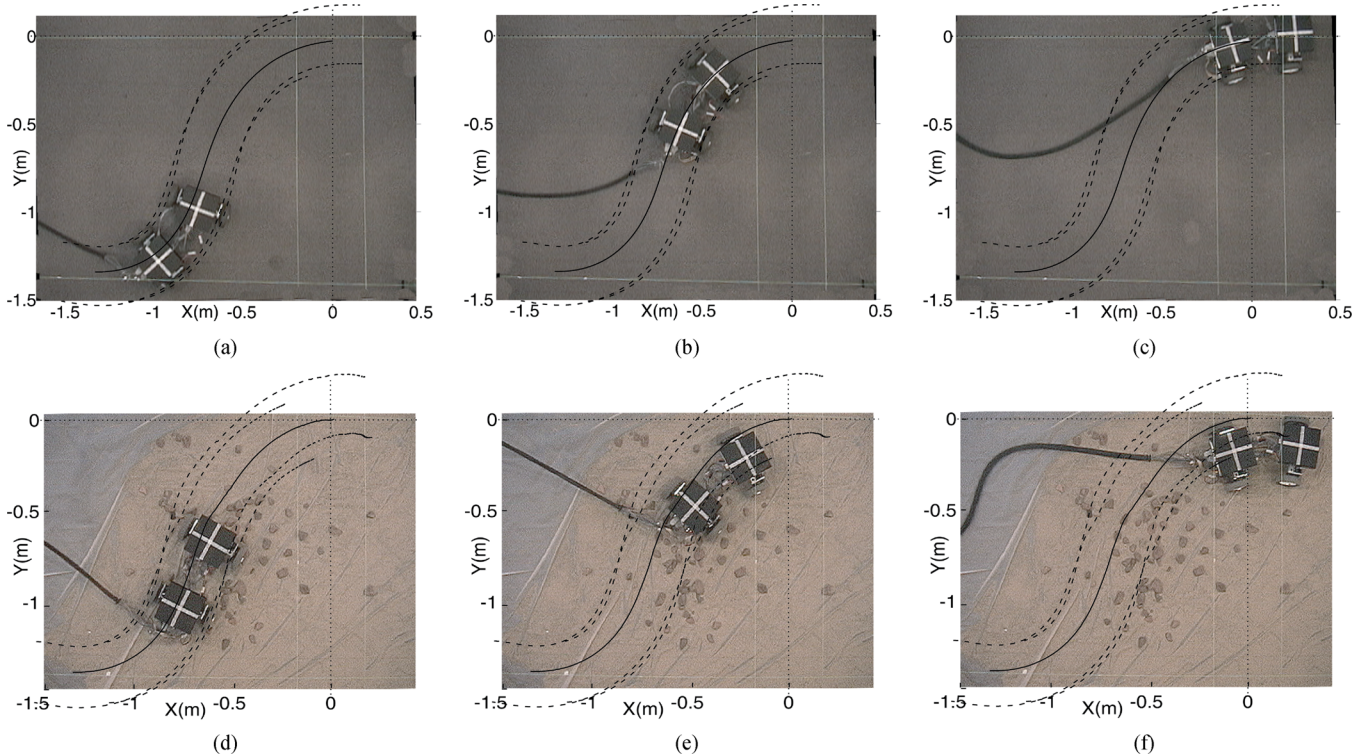


Fig. 6. Robot paths during posture regulation on carpet and on sand-and-rock. (a) $t = 4$ s (on carpet). (b) $t = 12$ s (on carpet). (c) $t = 60$ s (on carpet). (d) $t = 6$ s (on sand-and-rock). (e) $t = 12$ s (on sand-and-rock). (f) $t = 60$ s (on sand-and-rock).

sensing system, while a small amount of error results from the dynamic controller.

The nonideal kinematic motion controller with velocity feedback was used in Test 2. Compared to Test 1, E is increased by 121% and off-tracking Δ is increased by 1440% in Test 2. Velocity feedback also perturbed the kinematic motion controller and increased kinematic controller error (E_k , e_k^ϕ) significantly. Since the kinematic controller provides the reference trajectories to the dynamic controller, the dynamic control errors also became larger (E_d , e_d^ϕ). The posture errors were therefore increased significantly.

The nonrobust dynamic motion controller used in Test 3 also increased error and most of the trials failed. Position error E is 76% larger than Test 1. More importantly though, 60% of the trials failed to complete because the wheels collided during the maneuver due to off-tracking caused by nonrobustness of the controller. In the trials that did complete, the off-tracking is actually quite small, but this is NOT representative of this controller's performance. It is thus concluded that the system performance with nonrobust control is unreliable.

The sensor system is evaluated with just odometry feedback in Tests 4 and 6 on carpet and sand, respectively. Given the high traction provided by the carpet (Test 1), error E is only increased by 7% while off-tracking Δ is increased by 315%. This large increase in Δ illustrates the importance of the cooperative sensor. The sand surface (Test 6) underscores the importance of the cooperative sensing. Compared to Test 5, E is increased by 21% and Δ is increased by 822%, both with significantly increased standard deviations.

Fig. 6 shows the robot using the proposed architecture during posture regulation on carpet (Test 1) and sand-and-rock (Test 7). The white lines represent the string grids and the black lines represent sensor system data. The solid black line represents the predicted position of the middle point R and the dashed black lines represent estimated positions of the wheels. The system performs nearly as well with sand-and-rock as it did with the ideal high-traction carpet surface. This is a significant improvement over previous results without the proposed architecture, where error on sand-and-rock was as large as 66 cm [1]. Overall, all of these results demonstrate the superiority of the proposed distributed

cooperative motion control and sensing system to robustly maneuver nonideal terrain with significant disturbances.

The proposed architecture will be extended to multiaxle configurations (more than two axles) in future work. The architecture itself is quite generic and simply establishes the interaction amongst kinematic controllers, dynamic controllers, and sensory system components. Customization and extension of the algorithms within these components is currently being examined for this purpose.

VIII. CONCLUSION

This paper proposes a distributed cooperative motion control and sensing architecture combining a kinematic motion controller, a dynamic motion controller, and a sensor fusion system incorporating a relative position sensor for a two-axle Compliant Framed wheeled Modular Mobile Robot (CFMMR). Experimental results demonstrate the efficiency and robustness of the proposed technique. This motion control and sensing strategy is generally applicable to other cooperative mobile robots. Future work will focus on extending these results to other CFMMR configurations and improving performance of the sensing system and dynamic controller.

REFERENCES

- [1] M. A. Minor, B. Albiston, and C. Schwensen, "Simplified motion control of a two axle compliant framed wheeled mobile robot," *IEEE Trans. Robot.*, vol. 22, pp. 491–506, 2006.
- [2] X. Zhu, M. A. Minor, and S.-Y. Park, "Distributed robust control of compliant framed wheeled modular mobile robots," *ASME J. Dyn. Syst., Meas., Contr.*, vol. 128, no. 3, pp. 489–498, Sep. 2006.
- [3] H. Kimura and S. Hirose, "Development of Genbu: Active wheel passive joint articulated mobile robot," in *Proc. IROS'02*, Lausanne, Switzerland, Sep.–Oct. 2002, pp. 823–828.
- [4] H. Kimura, S. Hirose, and K. Shimizu, "Stuck evasion control for active-wheel passive-joint snake-like mobile robot "Genbu"," in *Proc. 2004 IEEE Int. Conf. Robot. Automat.*, New Orleans, LA, Apr.–May 2004, pp. 5087–5092.
- [5] B. W. Albiston and M. A. Minor, "Curvature based point stabilization for compliant framed wheeled modular mobile robots," in *Proc. IEEE ICRA*, Taipei, Taiwan, R.O.C., Sep. 2003, pp. 83–89.
- [6] A. Tayebi, M. Tadjine, and A. Rachid, "Invariant manifold approach for the stabilization of nonholonomic systems in chained form: Application to a car-like mobile robot," in *Proc. 1997 36th IEEE Conf. Decision Contr.*, San Diego, CA, Dec. 1997, pp. 4038–4043.
- [7] R. Fierro and F. L. Lewis, "Control of a nonholonomic mobile robot: Backstepping kinematics into dynamics," *J. Robot. Syst.*, vol. 14, pp. 149–163, 1997.
- [8] J.-M. Yang and J.-H. Kim, "Sliding mode motion control of nonholonomic mobile robots," *IEEE Contr. Syst. Mag.*, vol. 19, pp. 15–23, Apr. 1999.
- [9] M. Kumar and D. P. Garg, "Sensor-based estimation and control of forces and moments in multiple cooperative robots," *Trans. ASME J. Dynam. Syst., Meas. Contr.*, vol. 126, pp. 276–83, 2004.
- [10] Y. Hirata, Y. Kume, T. Sawada, Z.-D. Wang, and K. Kosuge, "Handling of an object by multiple mobile manipulators in coordination based on caster-like dynamics," in *Proc. IEEE ICRA'04*, New Orleans, LA, Apr.–May 2004, pp. 807–812.
- [11] C. P. Tang, R. Bhatt, and V. Krovi, "Decentralized kinematic control of payload transport by a system of mobile manipulators," in *Proc. IEEE ICRA'04*, New Orleans, LA, Apr.–May 2004, pp. 2462–2467.
- [12] A. Rodriguez-Angeles and H. Nijmeijer, "Mutual synchronization of robots via estimated state feedback: A cooperative approach," *IEEE Trans. Contr. Syst. Technol.*, vol. 12, no. 4, pp. 542–54, Jul. 2004.
- [13] A. G. O. Mutambara and H. E. Durrant-Whyte, "Estimation and control for a modular wheeled mobile robot," *IEEE Trans. Contr. Syst. Technol.*, vol. 8, no. 1, pp. 35–46, Jan. 2000.
- [14] H. G. Tanner, S. G. Loizou, and K. J. Kyriakopoulos, "Nonholonomic navigation and control of cooperating mobile manipulators," *IEEE Trans. Robot. Automat.*, vol. 19, no. 1, pp. 53–64, Feb. 2003.
- [15] K. Kosuge and M. Sato, "Transportation of a single object by multiple decentralized-controlled nonholonomic mobile robots," in *Proc. IROS'99: Human and Environment Friendly Robots with High Intelligence and Emotional Quotients*, Kyongju, Korea, Oct. 1999, pp. 1681–1686.
- [16] T. D. Murphrey and J. W. Burdick, "The power dissipation method and kinematic reducibility of multiple-model robotic systems," *IEEE Trans. Robot.*, vol. 22, no. 4, pp. 694–710, Aug. 2006.
- [17] X. Zhu, Y. Kim, and M. A. Minor, "Cooperative distributed robust control of modular mobile robots with bounded curvature and velocity," in *Proc. 2005 IEEE/ASME Int. Conf. Adv. Intell. Mechatron.*, Monterey, CA, 2005, pp. 1151–1157.
- [18] M. A. Minor and R. Merrell, "Instrumentation and algorithms for posture estimation in compliant framed modular mobile robotic systems," *Int. J. Robot. Res.*, vol. 26, no. 5, pp. 491–512, May 2007.
- [19] Y. Kim and M. A. Minor, "Decentralized kinematic motion control for multiple axle compliant framed modular wheeled mobile robots," in *Proc. IROS'06*, Beijing, China, Oct. 2006, pp. 392–397.
- [20] X. Zhu, R. Merrell, and M. A. Minor, "Motion control and sensing strategy for a two-axle compliant framed wheeled modular mobile robot," in *Proc. IEEE Int. Conf. Robot. Automat.*, Orlando, FL, 2006, pp. 3526–3531.
- [21] S. Park and M. A. Minor, "Modeling and dynamic control of compliant framed wheeled modular mobile robots," in *Proc. IEEE ICRA'04*, New Orleans, LA, Apr.–May 2004, pp. 3937–3943.